

# Microstructuring by two-photon polymerization using a sub-nanosecond laser

Raghwendra Kumar\* and S. Anantha Ramakrishna

Department of Physics, Indian Institute of Technology, Kanpur 208 016, India

**A multi-photon absorption-based laser writing system with sub-micrometer resolution has been developed using an inexpensive sub-nanosecond laser for two- and three-dimensional structuring in photosensitive resist materials. New combinations of commercially available photoresists such as SU-8 and AR-N 4340, and a photoinitiator (2, 4, diethyl-9H-thioxanten-9-one) with large two-photon absorption at 532 nm are shown to be effective in obtaining sub-micrometer line or dot resolution. Systematic studies of the resolution on the system and fabrication parameters such as laser power, writing speed, focusing arrangement, etc. have been carried out. The sub-nanosecond-based laser micro writer is an inexpensive alternative with similar capabilities as a femtosecond-based laser writer. This system is comparably effective and has much higher capabilities for 2D structuring in terms of the aspect ratio of the fabricated structures than conventional 2D laser micro writers.**

**Keywords:** Fabrication parameters, photoresists, sub-nanosecond laser, two-photon polymerization, writing system.

DURING the past few decades, several nano/micro fabrication techniques such as electron beam lithography (EBL), focused ion beam (FIB) milling and photolithography have been developed for the fabrication of simple as well as complex nano/microstructures<sup>1</sup>. Conventional laser writing and FIB milling have been only partially successful for fabrication of 3D micro/nanostructures. The need for vacuum using EBL and FIB methods can be disadvantageous. Micro-stereo lithography is an alternative method for 3D micro fabrication<sup>2</sup>, but has its limitations in terms of spatial resolution and writing speed. Multi-photon lithography can be highly advantageous over other techniques due to the localized nature of polymerization that can be employed for fabrication of highly complex 3D microstructures with spatial resolution far smaller than 100 nm using tightly focused beams beyond the diffraction limit<sup>3,4</sup>. This technique has found numerous applications in the fields of plasmonics<sup>5</sup>, memory devices<sup>6</sup>, photonic devices<sup>7</sup>, microelectromechanical systems (MEMS)<sup>8</sup> and chemical and biosensors<sup>9</sup>.

Much of multi-photon laser writing has been carried out using titanium: sapphire femtosecond lasers operating

at 780 nm wavelength. Although the ultrashort pulses are efficient for multi-photon polymerization, they are associated with high equipment cost. This can be offset by picosecond or sub-nanosecond lasers and using photoinitiators with large two-photon absorption cross-sections to obtain sub-wavelength resolution. He *et al.*<sup>10</sup> have reported a series of multi-photon absorbing materials that can be used for multi-photon polymerization using picosecond and sub-nanosecond lasers. Chung *et al.*<sup>11</sup> have reported 3D micro-structuring using a low-cost Q-switched Nd:YAG microlaser. Other groups have utilized hybrid organic-inorganic resist such as SZ2080 (ORMOSIL) for the fabrication of high-resolution structures with picosecond lasers. Also, 2,4-diethyl-9H-thioxanten-9-one was shown to effectively work as a photoinitiator with SZ2080 photoresist using 8 ps laser pulses<sup>12</sup>. These results clearly paved the way for low-cost fabrication systems and moving towards industrial rapid production<sup>13</sup>. We also note the single-photon absorption can be used for 3D micro-structuring with tightly focused beams at low intensity and the exposure threshold of photosensitive materials for fine development<sup>14</sup>. However, the writing speeds are comparatively small due to the long exposure times required.

Here, we present the development and optimization of a two-photon laser writing system using a sub-nanosecond laser operating at 532 nm wavelength and a combination of commercially available negative photoresists such as SU-8 and AR-N 4340 (refs 15, 16) and the photoinitiator (2,4-diethyl-9H-thioxanten-9-one). To the best of our knowledge, these combinations of photoresist and photoinitiator have not been reported so far. Systematic studies of resolution and dependence on laser power, and writing speed have been carried out for the fabrication of complex as well as simple microstructures. This system is competitive with those commercially available and based on expensive femtosecond lasers and proprietary photosensitive materials.

## Fundamentals of two-photon polymerization

### *Two-photon absorption and polymerization*

Two-photon absorption (TPA) is a nonlinear process where there is simultaneous absorption of two photons by

\*For correspondence. (e-mail: raghawk@iitk.ac.in)

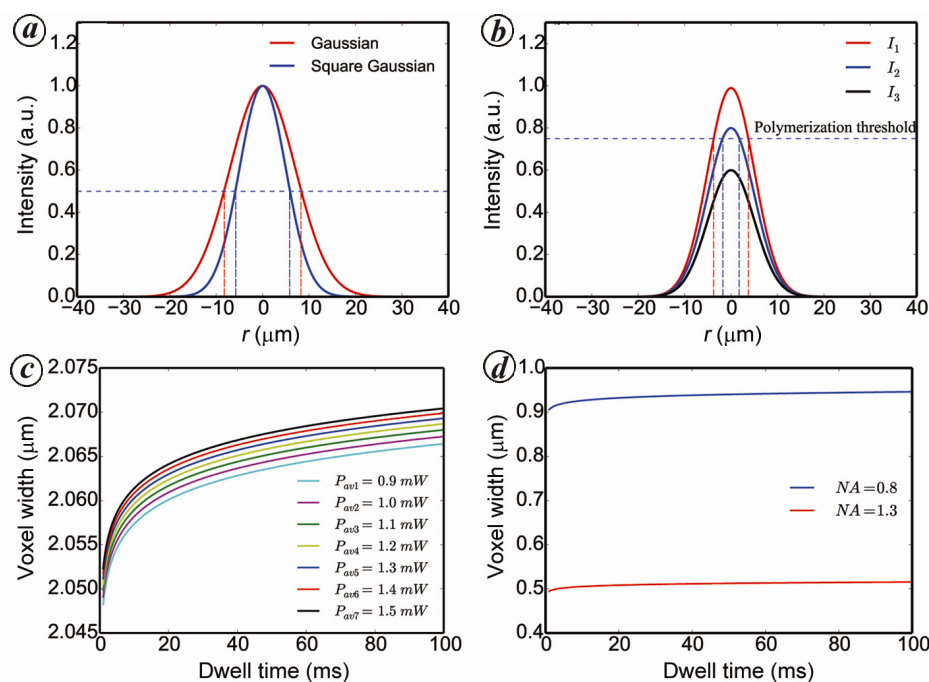


**Figure 1.** *a*, Comparison of the spatial full width at half maximum of a Gaussian shaped beam intensity and its squared ( $I^2$ ) profile. *b*, Schematic explaining a threshold intensity for photosensitive materials with a threshold assumed to be at horizontal dashed line. As the peak intensity gets closer to the threshold from above, the voxel width decreases. *c*, Evolution of voxel width with dwell time and average laser power. *d*, Change in voxel width with the numerical aperture (NA) of the objectives and dwell time. The parameters used to plot (*c*) and (*d*), i.e.  $\lambda$ , NA,  $n$ ,  $f$ ,  $P_{av}$ ,  $E_{th}$  are 532 nm, 0.8, 1.0, 10 kHz, 1.2 mW and  $6.6 \times 10^{-73}$  ( $\text{W}^2/\text{m}^4$ ) respectively.

atoms or molecules resulting in the molecule transitioning to an excited state. In this process, the rate of absorption is directly proportional to the square of the laser intensity it dominates only where the intensity is large enough. The energy absorption rate can be written as<sup>17</sup>

$$\frac{dW}{dt} = \frac{8\pi^2 h\omega}{c^2 n^2} I^2 \text{Im}[\chi^{(3)}], \quad (1)$$

where  $dW/dt$  is the change in energy per unit volume per unit time and  $\omega$ ,  $c$ ,  $n$ ,  $I$  and  $\chi^{(3)}$  are the angular frequency, speed of light in vacuum, refractive index of the medium, laser intensity and the third-order nonlinear optical susceptibility of the medium respectively.

A finely focused laser beam creates a 3D volume near the focal region where high laser intensity can be achieved. TPA can dominate over linear absorption and changes the properties of photosensitive materials within the focal volume. The area over which linear absorption causes change in the material is typically limited to the full width at half maximum (FWHM) of the laser beam. In contrast, the spatial feature size can be less than FWHM by a factor of  $\sqrt{2}$  due to the  $I^2$  dependence in case of TPA (Figure 1 *a*). Further, the material change and development processes require a minimum threshold dose of light, which may be used to restrict the region of changed material to sizes much smaller than the wavelength

(Figure 1 *b*). These are some of the characteristics that have made the two-photon laser writing technique appealing in the last few years.

Two-photon polymerization (TPP) is based on TPA, where a highly intense laser beam is tightly focused into the photosensitive material, which results in the formation of free monomer radicals. Such large intensities are typically obtained with femtosecond lasers in ordinary photosensitive materials. However, the inclusion of additional molecules with large TPA cross-sections in the monomer mix as photoinitiators can dramatically lower the threshold for TPP, where even sub-nanosecond laser pulses can cause polymerization or cross-linking. These monomer radicals react with other monomers through a polymerization chain reaction until two such monomer radicals meet and finally terminate as a polymer<sup>18</sup>.

### Theoretical estimation of voxel dimensions

A voxel is defined as the unit element of a three-dimensional object in a manner similar to the pixel of a two-dimensional picture. In the case of TPP, the voxel dimensions depend on a number of fabrication conditions and system parameters such as laser power, pulse repetition rate, pulse width, exposure time, numerical aperture (NA) of the focusing lens and the TPA cross-section of photosensitive materials. Due to the threshold intensity

that is required to form a stable structure, the polymerization threshold can be estimated as

$$I_{th}^2 \beta \tau f t \geq E_{th}, \quad (2)$$

where  $I_{th}$ ,  $\tau$ ,  $f$ ,  $t$ ,  $\beta$  and  $E_{th}$  are the threshold laser intensity, pulsed duration, repetition rate, dwell time, absorption coefficient of photosensitive material and threshold energy per unit volume respectively.

The intensity distribution of a Gaussian laser beam is

$$I(r, z) = \frac{2P}{\pi w(z)^2} \exp \left[ -2 \left( \frac{r}{w(z)} \right)^2 \right], \quad (3)$$

where the amplitude is defined as  $I(z) = 2P/[\pi w(z)^2]$ , where  $P$  is the average laser power,  $w(z)$  the spot radius at the  $z$  plane and  $r = \sqrt{x^2 + y^2}$  is the radial coordinate in the  $x$ - $y$  plane.

At the focal plane ( $z = 0$ ), we define  $I_0 = I(z = 0)$  and  $w_0 = w(z = 0)$  at the beam waist. The beam width elsewhere is

$$w(z) = \frac{\lambda}{\pi \tan \left[ \sin^{-1} \left( \frac{NA}{n} \right) \right]} \left[ 1 + \left( \frac{z\lambda}{\pi w_0^2} \right)^2 \right]^{1/2}, \quad (4)$$

where  $n$  is the refractive index of the medium,  $\lambda$  the wavelength and NA is the numerical aperture of the lens used to focus the beam. The voxel width ( $D$ ) and voxel depth ( $L$ ) along the beam direction can be obtained from eqs (2)–(4) as

$$D(t, NA, P_{av}, f) = \frac{\lambda}{\pi \tan \left[ \sin^{-1} \left( \frac{NA}{n} \right) \right]} \times \left[ \ln \left( \frac{4\pi^2 P_{av}^2 f t \left[ \tan \left( \sin^{-1} \left( \frac{NA}{n} \right) \right) \right]^4}{\lambda^4 E'_{th}} \right) \right]^{1/2}, \quad (5)$$

$$L(t, NA, P_{av}, f) = \frac{2\lambda}{\pi \tan \left[ \sin^{-1} \left( \frac{NA}{n} \right) \right]} \times \left[ \left( \frac{4\pi^2 P_{av}^2 f t \left[ \tan \left( \sin^{-1} \left( \frac{NA}{n} \right) \right) \right]^4}{\lambda^4 E'_{th}} \right)^{1/2} - 1 \right]^{1/2}, \quad (6)$$

where  $E'_{th} = E_{th}/[\beta\tau]$ . and  $D$ ,  $L$  are voxel width, voxel depth respectively. Since the writing speed of the stage is

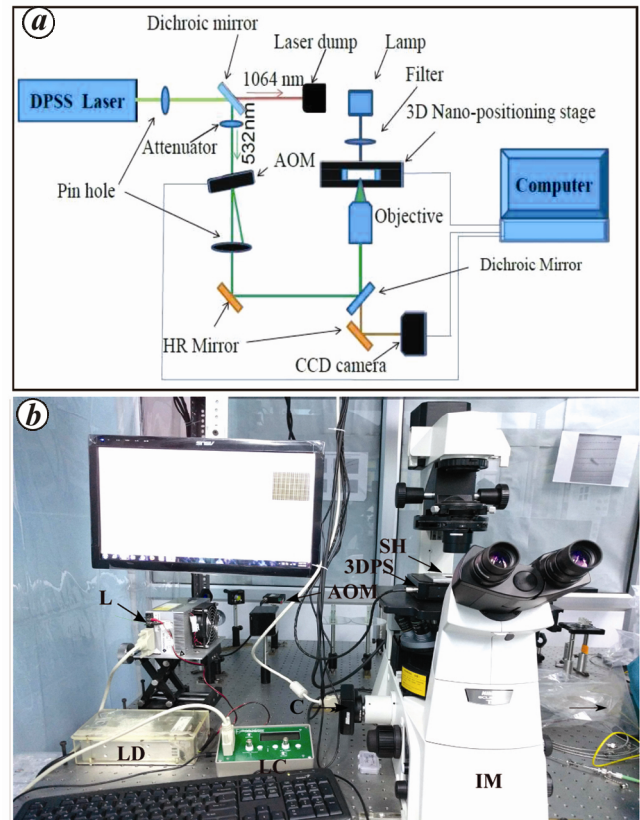
inversely proportional to the beam dwell time at a point, the dependence of voxel dimensions on the writing speed can be obtained by replacing the dwell time with the inverse of stage speed multiplied by the spot size in the eq. (5).

Figure 1 *c* and *d* shows the dependence of voxel width on dwell time and NA of the focusing lens respectively, as predicted by eq. (5). Figure 1 *d* clearly shows that high resolution can be obtained using a high NA objective. Figure 1 *c* shows that the focusing parameters and dwell time are more critical to obtain a small voxel dimension than the laser power due to the fine focusing conditions here. Thus, the theoretical predictions clearly show that high spatial localization of a voxel can be obtained using precise control over the laser power just above the polymerization threshold for less than 20 ms dwell times and 1 mW of average laser power.

## Equipment and materials

### Two-photon laser writing system

Figure 2 *a* is a schematic diagram of the laser writing system. It comprises a sub-nanosecond laser of 700 ps



**Figure 2.** *a*, Schematic diagram of the two-photon laser writing system. *b*, Photograph of the same system where L is the sub-nanosecond laser, LD is laser driver, LC is laser controller, IM is inverted microscope, C is CCD camera, AOM is AO modulator, 3DPS is 3D piezo nano positioning stage and SH is sample holder.

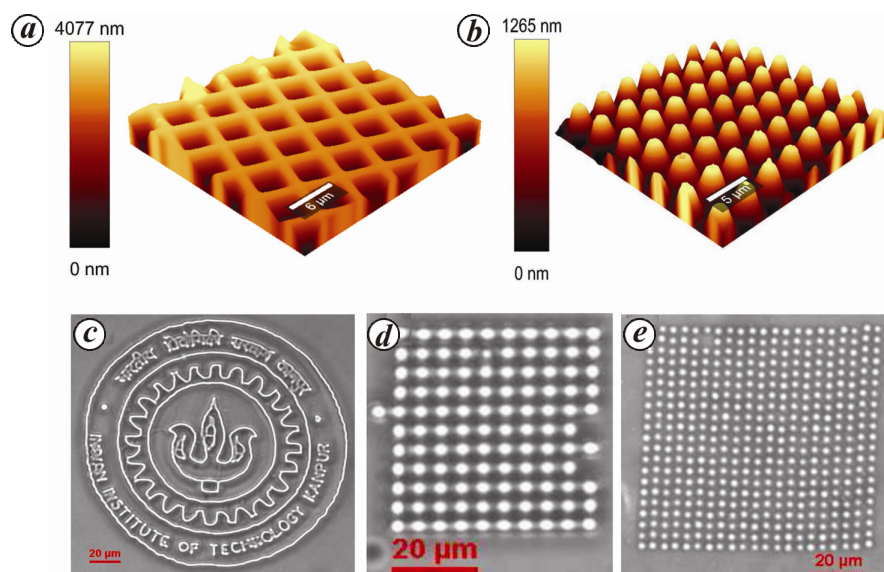


**Figure 3.** *a, b*, 3D view of AFM topographical images of a 2D grating and a 2D micro disk array respectively. *c–e*, Optical microscopy images of logo of IIT Kanpur, an array of micro pillars of height 6  $\mu\text{m}$  and a 2D disk array respectively. (*a–d*) are fabricated in SU-8, while (*e*) is fabricated in AR-N 4340. All these microstructures are fabricated using the parameters: 1.2 mW laser average power, 100  $\mu\text{m}/\text{s}$  writing speed, 10 kHz rep rate and 0.8 NA objective.

pulse width (Wedge\_532\_1064, Bright Solutions, Italy), with simultaneous output at 532 and 1064 nm wavelengths. A piezoelectric XYZ (3D) nano-positioning stage (PI E-725, Physik Instrumente, Germany) with a travel range of 200  $\mu\text{m} \times 200 \mu\text{m} \times 200 \mu\text{m}$ , and 0.5 nm closed-loop resolution is mounted on an inverted microscope (Eclipse Ti-s, Nikon) with high NA (50 and 100X) objectives. An acoustic-optic modulator (AOM; IntraAction Corp., USA) and other optical components are used for guiding the laser beam up to the sample holder mounted on the piezo stage. All components are mounted on a floating vibration-free table (Newport Corp., USA) to prevent vibrational disturbances during fabrication. The entire set-up is interfaced through LabView software, which is used to simultaneously control the motion of the piezoelectric stage as well as the AOM. The user interface accepts data in the form of Cartesian coordinates specified in a text format. The design of structures is done using a computer-aided design (CAD) software and coordinates are extracted in Cartesian format for loading into the LabView program.

A dichroic mirror is used here to reject the laser output at 1064 nm and use only the 532 nm radiation. The AOM is aligned at the Bragg angle to diffract the beam into three components (−1, 0, 1) with a pinhole that selects the first-order (+1) diffracted beam. This beam is guided into the microscope turret and the objective by a high-reflection mirror and focused at sample holder by objective. The sample holder is placed on the 3D nano-positioning stage. A camera is used to view the samples through a dichroic mirror for observation of the writing process. Figure 2 *a* and *b* shows schematic diagram and photograph of the two-photon laser writing system respectively.

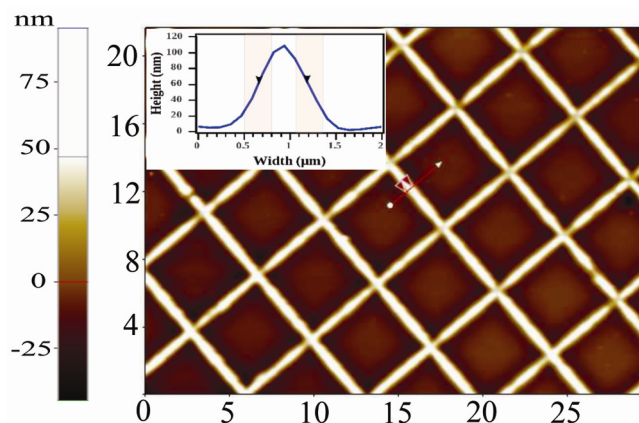


**Figure 4.** AFM topographical image of a 2D grating fabricated using 100X oil immersion objective in SU-8. (Inset) The corresponding line profile of selected portion of the line. FWHM of the corresponding line profile is around 500 nm.

### Photosensitive materials

Usually the photosensitive materials reported by researchers who have used sub-nanosecond lasers are proprietary in nature<sup>12</sup>. We used commercially available negative photoresists SU-8-3005 (MicroChem Corp., USA) and AR-N 4340 (Allresist, Germany). SU-8 has an optimum cross-linking response in the wavelength range 350–400 nm. AR-N 4340 has an optimum response in the wavelength range 300–390 nm, specially for the Hg i-line and also responds to the deep-UV (248–265 nm) and g-line (436 nm) as well. Thus, AR-N 4340 shows extremely good response for polymerization by TPA at 532 nm and can be used even without a photoinitiator.



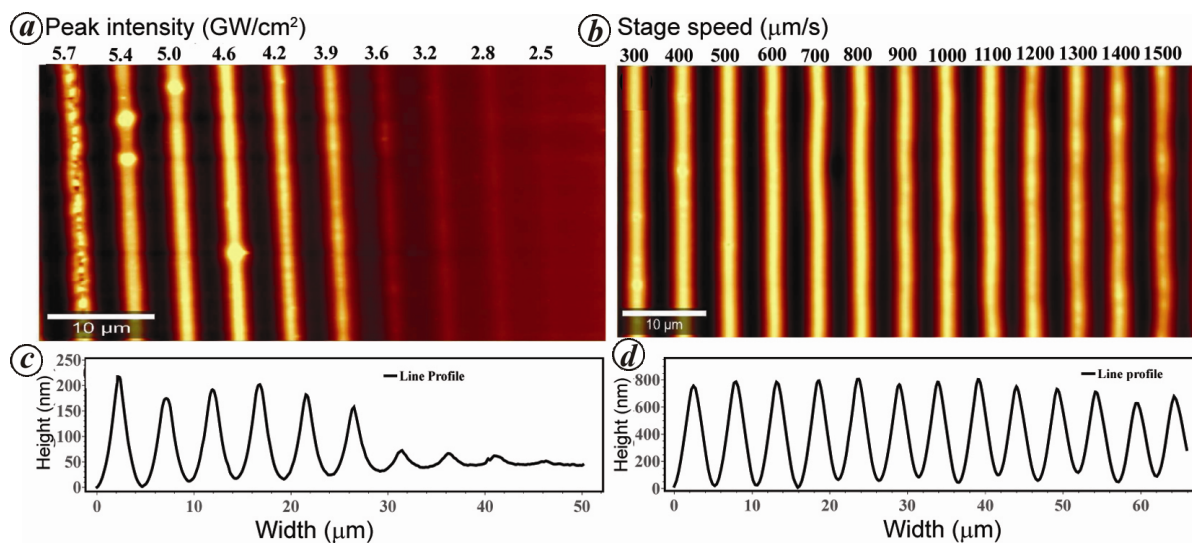


**Figure 5.** *a*, AFM topographical image of micro lines array fabricated in SU-8 at constant writing speed  $100 \mu\text{m/s}$  with decreasing peak intensity of  $5.7 \text{ GW/cm}^2$  to  $2.5 \text{ GW/cm}^2$  (from left to right). *b*, Micro lines array fabricated in SU-8 at constant peak intensity  $4.6 \text{ GW/cm}^2$  with increasing writing speed of  $300$  to  $1600 \mu\text{m/s}$  (from left to right). *c*, *d*, Corresponding line profiles of (*a*) and (*b*) respectively.

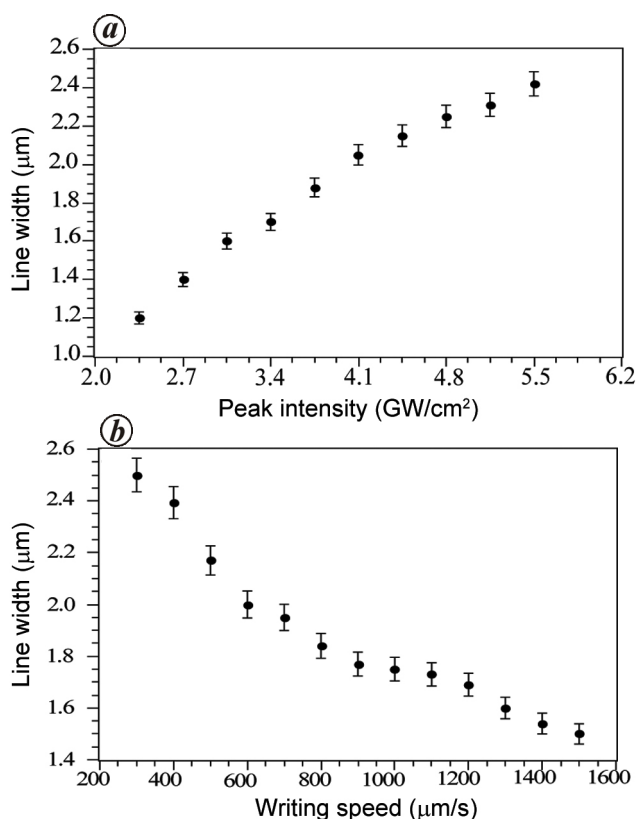


**Figure 6 a, b.** Line width (of Figure 5 *a* and *b*) as a function of peak intensity and writing speed respectively. Data points represent FWHM of line profiles, while error bars show the variance in line width.

The photoinitiator (2,4-diethyl-9H-thioxanten-9-one) which has an absorption maximum at  $255 \text{ nm}$  (ref. 13) was used with the given photoresists to enhance the TPA

at  $532 \text{ nm}$  wavelength. The amount of photoinitiator used here is typically 3% by weight of the photoresist.

#### Fabrication of microstructures in SU-8 and AR-N 4340

Generally SU-8 shows poor adhesion with glass substrate. So HMDS (hexamethyldisilazane) was used as a promoter to enhance adhesion with the glass substrate. Thoroughly cleaned glass substrates were coated with a thin layer of HMDS at  $6000 \text{ RPM}$  for  $45 \text{ sec}$  and baked on a hotplate at  $120^\circ\text{C}$  for  $2 \text{ min}$ . After cooling, the mixture of SU-8 and photoinitiator was coated at  $2000 \text{ RPM}$  for  $1 \text{ min}$ , pre-baked at  $65^\circ\text{C}$  for  $2 \text{ min}$  and at  $95^\circ\text{C}$  for  $3 \text{ min}$ , and finally exposed to light under the laser writing system operating at  $532 \text{ nm}$  wavelength. After post-exposure bakes carried out for  $3 \text{ min}$  at  $65^\circ\text{C}$  and  $5 \text{ min}$  at  $95^\circ\text{C}$ , the exposed portions get hardened. After cooling to room temperature, development of the polymerized structures was carried out in propylene glycol methyl ether acetate for  $20 \text{ sec}$ , followed by washing in isopropyl alcohol for  $1 \text{ min}$ . During development the unexposed portions get washed away leaving behind the cross-linked structure. Development time depends on the thickness of the coated material, and it is typically longer for thicker photoresists.

Fabrication of microstructures in AR-N 4340 was carried out as follows: cleaned glass substrates were coated with AR-N 4340 photoresist at  $2000 \text{ RPM}$  for  $1 \text{ min}$ , pre-baked at  $85^\circ\text{C}$  for  $2 \text{ min}$  and exposed to light under the laser writing system. After post-exposure bake carried out for  $5 \text{ min}$  at  $95^\circ\text{C}$ , the exposed portions get hardened. After cooling down to room temperature, development of

the polymerized structures was carried out in AR-300-475 for 20 sec, followed by washing in DI water for 1 min.

Figure 3 *a* and *c* shows the 3D view of atomic force microscopy (AFM) images of a 2D grating and a 2D disk array. Control of the stage motion can enable formation of complex micro structures: for example, Figure 3 *c* and *d* shows the optical microscopy images of the logo of IIT Kanpur and an array of 3D pillars fabricated in SU-8 photoresist. Figure 3 *e* shows the 2D disk array fabricated in AR-N 4340 photoresist. These microstructures (Figure 3 *a–e*) were fabricated using the following parameters: 1.2 mW laser average power, 100  $\mu\text{m/s}$  writing speed, 10 kHz rep rate and 0.8 NA objective. Resolution of the fabricated structures highly depends on the NA of the objective. We used a 100X oil immersion objective with 1.3 NA for fabricating the microstructures and obtained spatial resolution around 500 nm for well-defined lines (inset, Figure 4). This 2D grating is fabricated in SU-8 using the following parameters: 1.0 mW laser average power, 200  $\mu\text{m/s}$  writing speed, 10 kHz rep rate and 1.3 NA oil immersion objective.

### Characterization and calibration of microstructures

AFM (Alpha 300 RAS, WITec, Germany) and optical microscopy (Eclipse Ti-s, Nikon) were used to characterize the microstructures. AFM was used in non-contact mode with pyramidal-shaped tips (radius  $<10$  nm). We studied experimentally the effects of laser peak intensity, writing speed and dwell time on the width of micro lines (Figure 5). It was noticed that the width of micro lines increases with increasing dwell time and peak intensity, which validates the theoretical prediction (Figure 1 *c*). Damage to the photosensitive resin at higher laser powers can be seen in the first two lines (from left in Figure 5 *a*). For less than the threshold pulse energy, definition of the line is not complete. Thus, a fine control over the peak intensity is necessary. We also checked the effect of writing speed on the line width and it matched quite well with the theoretical prediction (Figure 5 *b*). Figure 5 *a* and 5 *b* shows AFM topographical images of the micro lines, fabricated at different peak intensities and writing speeds respectively. At very high writing speeds (lines on the right), the lines have a smooth, rounded profile with smaller heights (Figure 5 *b*). Figure 5 *c* and *b* shows the corresponding height profiles of the lines drawn at various laser peak intensities and writing speeds respectively. Figure 6 *a* and *b* shows the measured line widths (FWHM) versus peak intensity and writing speed respectively. The width of the fourth micro-line from the left in Figure 5 *b* was used along with the fabrication parameters to fit  $E'_{\text{th}}$  in eq. (5) (ref. 19). The fabrication parameters of the micro-line i.e.  $\lambda$ , NA,  $n$ ,  $f$ ,  $P_{\text{av}}$ ,  $E'_{\text{th}}$  are 532 nm, 0.8, 1.0, 10 kHz 1.2 mW and  $6.6 \times 10^{-73}$  ( $\text{W}^2/\text{m}^4$ ) respectively.

The fitted value of  $E'_{\text{th}}$  ( $6.6 \times 10^{-73}$   $\text{W}^2/\text{m}^4$ ) was used to plot Figure 1 *c* and *d*. The theoretical fits describe the observed trends in Figure 5 very well.

### Conclusion

A two-photon 3D laser writing system with sub-micrometer resolution based on sub-nanosecond pulsed laser has been developed. We studied and optimized the effects of different processing parameters such as average laser power, writing speed and laser spot dwell time on the line width of the microstructures. We used SU-8 and AR-N 4340 photoresists with a combination of photoinitiator (2,4-diethyl-9H-thioxanten-9-one) that has large two-photon absorption cross-section at wavelength 532 nm. Line resolution as small as about 0.5  $\mu\text{m}$  (FWHM) has been demonstrated as well as 3D pillars of about 6  $\mu\text{m}$  height. AR-N 4340 by itself has large enough TPA for laser structuring by TPP even without the addition of a photoinitiator. The system based on an inexpensive sub-nanosecond laser and commercially available photoresist materials promises to be an inexpensive substitute for expensive femtosecond laser-based writers. It also has much higher capabilities for 2D microstructuring in terms of aspect ratio than conventional 2D laser micro writers.

1. Lee, K.-S., Kim, R. H., Yang D.-Y. and Park, S. H., Advances in 3D nano/microfabrication using two-photon initiated polymerization. *Prog. Polym. Sci.*, 2008, **33**, 631–681.
2. Goswami, A., Phani, A., Umarji, A. M. and Madras, G., Polymer microfabrication by scanning based micro stereolithography: optical design and material functionality. *Rev. Sci. Instrum.*, 2012, **83**, 095003.
3. Kawata, S., Sun, H.-B., Tanaka, T. and Takada, K., Finer features for functional micro devices. *Nature*, 2001, **412**, 697–698.
4. Emons, M., Obata, K., Binhammer, T., Ovsianikov, A., Chichkov, B. N. and Morgner, U., Two-photon polymerization technique with sub-50 nm resolution by sub-10 fs laser pulses. *Opt. Mater. Express*, 2012, **2**, 942–947.
5. Reinhardt, C., Kiyon, R., Passinger, S., Stepanov, A. L., Ostendorf, A. and Chichkov, B. N., Rapid laser prototyping of plasmonic components. *Appl. Phys. A*, 2007, **89**, 321–325.
6. Cumpston, B. H. *et al.*, Two-photon polymerization initiators for three-dimensional optical data storage and microfabrication. *Nature*, 1999, **398**, 51–54.
7. Farsari, M. and Chichkov, B. N., Materials processing: two-photon fabrication. *Nature Photonics*, 2009, **3**, 450–452.
8. Schizas, C. *et al.*, On the design and fabrication by two-photon polymerization of a readily assembled micro-valve. *Int. J. Adv. Manuf. Technol.*, 2009, **48**, 435–441.
9. Doraiswamy, A. *et al.*, Two photon induced polymerization of organic inorganic hybrid biomaterials for microstructured medical devices. *Acta Biomater.*, 2006, **2**, 267–275.
10. He, G. S., Tan, L.-S., Zheng, Q. and Prasad, P. N., Multiphoton absorbing materials: molecular designs, characterizations and applications. *Chem. Rev.*, 2008, **108**, 1245–1330.
11. Chung, T.-T., Li Tseng, C., Hung, C.-P., Lin, C.-L. and Baldeck, P. L., Design and two-photon polymerization of complex functional micro-objects for lab-on-a-chip: rotating micro-valves. *J. Neurosci. Neuroeng.*, 2013, **2**, 1–5.

## RESEARCH ARTICLES

---

12. Malinauskas, M., Danilevicius, P. and Juodkazis, S., Three-dimensional micro-/nano-structuring via direct write polymerization with picosecond laser pulses. *Opt. Express*, 2011, **19**, 5602–5610.
13. Malinauskas, M., Purlys, V., Rutkauskas, M. and Gadonas, R., Two-photon polymerization for fabrication of three-dimensional micro- and nanostructures over a large area. *Proc. SPIE*, 2009, **7204**, 72040C–72040C-11.
14. Thiel, M., Fischer, J., von Freymann, G. and Wegener, M., Direct laser writing of three-dimensional submicron structures using a continuous-wave laser at 532 nm. *Appl. Phys. Lett.*, 2010, **97**, 221102.
15. del Campo, A. and Greiner, C., SU-8: a photoresist for high-aspect-ratio and 3D submicron lithography. *J. Micromech. Microeng.*, 2007, **17**, R81–R95.
16. Cao, H.-Z., Zheng, M.-L., Zi Dong, X., Zhao, Z.-S. and Duan, X.-M., Direct writing of shape-controlled nanodot array by two-photon nanolithography using elliptical beam. *Appl. Phys. Express*, 2013, **6**, 066501.
17. Boyd, R. W., *Nonlinear Optics*, Academic Press, Burlington, 2008, 3rd edn, pp. 556–558.
18. Leatherdale, C. A., DeVoe, R. J., Yeates, A. T., Belfield, K. D., Kajzar, F. and Lawson, C. M., *SPIE Proc. Ser.*, 2003, **5211**, 112–123.
19. Liu, Y., Nolte, D. D. and Nolte, L. J. P., Large-format fabrication by two-photon polymerization in SU-8. *Appl. Phys. A*, 2010, **100**, 181–191.

ACKNOWLEDGEMENTS. We thank Defence Research and Development Organization, New Delhi for providing funds (grant no. DECS/15/15124/D(R& D)/CARS-1) and Dr Sriram Guddala (IIT Kanpur) for useful discussions. R.K. gratefully thanks Council of Scientific and Industrial Research, New Delhi for fellowship. S.A.R. thanks DST, New Delhi for partial funding (grant no. DST/STF/PSA01/2011-2012).

Received 26 July 2016; revised accepted 21 November 2016

doi: 10.18520/cs/v112/i08/1668-1674

---